hundreds to thousands of meters of ice can be deposited in some locations (*9*).

Recent geological mapping shows features at low latitudes best interpreted as glacial in origin (see the figure). Features occur in isolated low-latitude locations such as the flanks of the Tharsis volcanoes that are reminiscent of moraines, knobs formed as a residual similar to terrestrial water-ice sublimation hills, and flow-line morphology (*10*). Remarkably, these are the same locations for which dynamical models show preferential deposition of water ice (*9*).

Thus, the geological evidence supports the dramatic climate changes that would be induced by the changing obliquity. Indeed, large changes in the climate appear to be the natural consequence of the temporal oscillations of the system.

Surface features and geomorphology can also tell us much about the ancient climate. The occurrence of valley networks on the oldest surfaces and high erosion rates inferred from crater degradation and removal have long argued for a warmer and wetter environment on Mars earlier than about 3.7 billion years ago. The Sun was 30% less luminous then than it is today, increasing the greenhouse warming required to raise temperatures enough to allow liquid water. A thick CO_2 greenhouse atmosphere would have saturated at temperatures that were still too low, making a martian greenhouse problematic (*11*), and the radiative effects of dust or clouds may not have alleviated this problem (*12*). Impacts at the end of planetary formation may have mobilized water for brief periods, producing rainfall that might have formed the valley networks without requiring a sustained greenhouse (*13*). However, the timing of large impacts, the long tail in the decline of moderate-sized impacts and their climatic effects, and the requisite thickness of the atmosphere still need to be better understood.

Recent spacecraft results provide important new constraints on the history of liquid water. The Meridiani landing site for Opportunity has sulfate-rich deposits that require liquid water to have been present for sufficiently long times to have had significant geochemical effects (*14*). Mapping of these deposits from orbit (*15*, *16*) shows that they occur as regional rather than local deposits. Thus, the conditions allowing liquid water likely were produced by global rather than local conditions. In addition, clay minerals that are indicative of chemical weathering in the presence of liquid water occur only on the ancient surfaces (*16*).

These new results appear to have required the prolonged occurrence of liquid water during the early epochs. One possible mechanism is a relaxation of the constraints imposed by the faint young Sun (*17*). The early Sun would have been more luminous if it had been even slightly more massive; subsequent mass loss would have brought the Sun to its current mass. Allowable values of the early Sun's luminosity require less greenhouse warming, and a CO_2 greenhouse atmosphere is plausible. The measurements are few and the uncertainties large, however (*18*). And, if the faint young Sun problem is mitigated, the role of impacts in also mobilizing water is unclear.

The changes in our understanding of martian history and implications for climate and volatile evolution are not just minor tweaking of existing hypotheses; rather, they are changing our view of what the important processes have been. Admittedly, much uncertainty still surrounds the nature of the earliest climate and of the processes responsible for controlling it are still very uncertain. On the obliquity and the seasonal time scales, though, the evidence is both compelling and dramatic. As the history of liquid water is written in Mars' geological history, these new results, when properly digested, will be important for deciphering Mars' biological potential.

References

1. Planet Mars II workshop, Les Houches, France, 23 May to 1 June 2005.
2. P. C. Thomas *et al.*, *Icarus* **174**, 535 (2005).
3. J. P. Bibring *et al.*, *Nature* **428**, 627 (2004).
4. A. Colaprete *et al.*, *Nature* **435**, 184 (2005).
5. M. T. Mellon, B. M. Jakosky, *J. Geophys. Res.* **100**, 11781 (1995).
6. J. F. Mustard, C. D. Cooper, J. F. Rifkin, *Nature* **412**, 411 (2001).
7. J. Laskar *et al.*, *Icarus* **170**, 343 (2004).
8. B. M. Jakosky *et al.*, *Astrobiology* **3**, 343 (2003).
9. B. Levrard *et al.*, *Nature* **431**, 1072 (2004).
10. D. E. Shean, J. W. Head, D. R. Marchant, *J. Geophys. Res.* **110**, 10.1029/2004JE002360 (2005).
11. J. F. Kasting, *Icarus* **94**, 1 (1991).
12. F. Forget, R. T. Pierrehumbert, *Science* **278**, 1273 (1997).
13. T. L. Segura O. B. Toon, A. Colaprete, K. Zahnle, *Science* **298**, 1977 (2002).
14. S. W. Squyres *et al.*, *Science* **306**, 1709 (2004).
15. B. M. Hynek, *Nature* **431**, 156 (2004).
16. J. P. Bibring *et al.*, *Science* **307**, 1576 (2005).
17. I. J. Sackmann, A. I. Boothroyd, *Astrophys. J.* **583**, 1024 (2003).
18. B. E. Wood *et al.*, *Astrophys. J.* **628**, L143 (2005).

10.1126/science.1118031

GEOPHYSICS

The Ghost of an Earthquake

William C. Hammond

Unlike the shadowy remains of departed souls, past earthquakes can leave traces that are detectable today with modern geophysical instrumentation. If large enough, a seismic event in the upper crust (less than about 15-km depth) can change the state of stress in the Earth to mantle depths (depths greater than about 30 km. These stresses subsequently relax over time scales of weeks to decades. The length of time needed to fully equilibrate depends on the material properties of the lower crust and upper mantle, and the size and style of the earthquake. On page 1473 of this issue, Gourmelen and Amelung (*1*) report evidence that relaxation following large earthquakes in the early to mid-20th century is presently observable in central Nevada. Because it is transitory, the presence of this signal has profound implications for our interpretation of geodetic data with respect to crustal deformation in the western United States.

Enhanced online at www.sciencemag.org/cgi/content/full/310/5753/1440

The author is at the Nevada Bureau of Mines and Geology, University of Nevada, Reno, Reno NV 89557–0088, USA. E-mail: whammond@unr.edu

When subjected to loads, Earth's deep layers are thought to behave viscoelastically. Viscoelastic materials exhibit a component of viscous flow in their response to stress, in addition to an instantaneous (elastic) deformation. Therefore the response to an instantaneous stress change is drawn out in time, and in the specific case of Maxwell viscoelasticity used by Gourmelen and Amelung (*1*), decreases with time toward zero. Loads of sufficient size include sudden stress changes that occur in earthquakes (*2*), or the more gradual and/or time-variable loading owing to removal of continental ice sheets (*3*), or draining of large Pleistocene lakes (*4*, *5*).

Identifying and correcting for postseismic effects may be necessary when geodetic measurements, such as those that are frequently made with the Global Positioning System (GPS), are used to map the slow, inexorable motion of tectonic blocks. Such measurements have helped show that the Basin and Range province of the interior western United States is a part of the wide (~1000 km) and diffuse plate boundary deformation zone that accommodates the relative motion between the Pacific and North American plates (*6*). In these regions, GPS measurements are used to quantify seismic hazard by estimating deformation rates near active faults. Thus, the existence of transient deformation features that are hundreds of kilometers wide, with deformation rates up to several millimeters per

year, is of considerable interest. Because transient effects do not represent the time-invariant fault loading that is typically assumed in seismic hazard assessment studies, these effects must be estimated and removed. The figure shows the predicted magnitude and direction of horizontal velocity that the 20th-century earthquakes in central Nevada could have (*7*), according to the Gourmelen and Amelung model (*1*) and relaxation theory (*8*). The maximum predicted change in velocity is ~2.5 mm year^{-1} across the location of the Pleasant Valley 1915 rupture, an effect that is quite large when considering that the total relative motion across the western Great Basin is ~10 mm year^{-1}. However, distinguishing the horizontal relaxation from the background secular deformation of the Basin and Range is difficult because the two fields are superimposed.

The validity of the model and the correction that it implies are supported by a comparison between paleoseismically and geodetically inferred slip rates on the faults that activated during the 20th-century Nevada earthquakes. These slip rates independently obtained by geodesy and paleoseismic techniques disagree to a level well outside the uncertainties in those techniques (*9*). Theoretically, however, slip rates obtained by geologic means (i.e., through estimating the size, style, and history of markers offset by earthquake rupture) should be in rough agreement with rates inferred by geodetic measurement. This explicitly assumes that geodesy measures crustal strain accumulation that is followed by episodic seismic release in earthquakes, and that the slip rate is approximately constant over time. In reality, both of these assumptions can be in error. In some cases, fault slip rates have been inferred to change over time [see, for example, (*10*, *11*)]. Alternatively, as in the case of central Nevada, the geodetic field can be "contaminated" by viscoelastic aftereffects, giving the false impression of slip rate disagreement. Crucial to the plausibility of the relaxation model presented by Gourmelen and Amelung (*1*) is the fact that it explains this discrepancy extremely well by reducing the amount of the geodetic deformation attributable to the steady time-invariant motion of tectonic blocks.

The Gourmelen and Amelung results (*1*) contribute directly to a longstanding debate over the location of strength in the continental lithosphere. The Interferometric Synthetic Aperture Radar (InSAR) data, provide very high resolution images of surface changes over time. Using these data, they infer that the Basin and Range lower crust has higher viscosity than the upper mantle, a result that agrees with studies

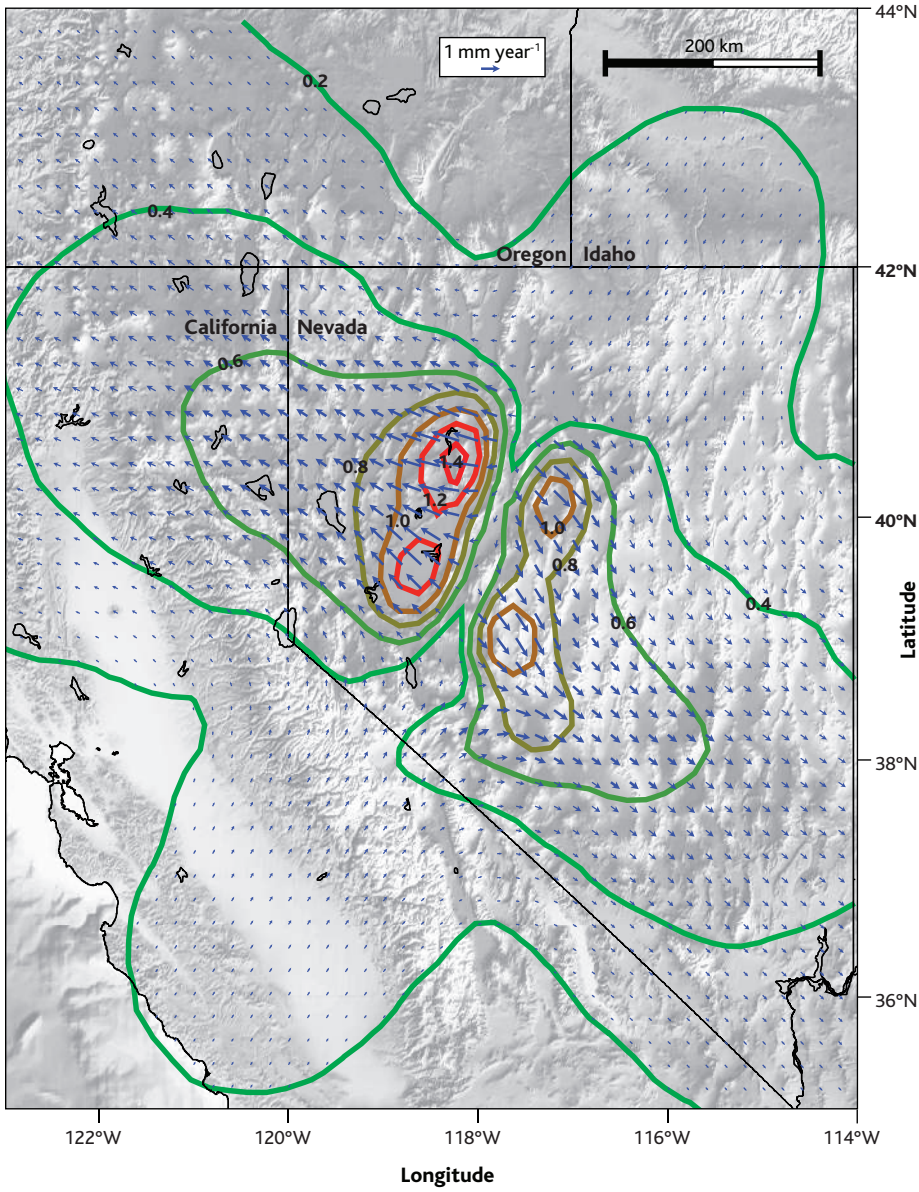

Postseismic relaxation. Contours show the magnitude, and vectors (blue) show the horizontal velocity, of surface motion (in millimeters per year) from the model of postseismic relaxation that is consistent with InSAR and GPS data (*1*, *7*). In contrast to the vertical motion that is focused within ~100 km of the seismic events (*1*), the horizontal component extends many hundreds of kilometers from the epicenters, but is more difficult to distinguish from the background secular deformation. Velocity is with respect to the central Nevada seismic belt faults, which are located approximately between the lobes of rapid postseismic motion (*1*).

based on modeling geodetic data obtained after earthquakes, and Pleistocene lake unloading. However, it is in disagreement with other studies that suggest that the lower crust may be weaker than the mantle (*12*) owing to compositional differences (*13*), or the need to explain the presence of metamorphic core complexes (*14*). The vertical position of this strength is important because it determines the extent to which the geometry and orientation of crustal blocks control deformation of the North America plate. Strength residing in the uppermost crust implies lithospheric deformation controlled by friction on faults. However, if the strength resides primarily in deeper layers, then the crustal blocks delineated by surface faulting are reacting passively to stresses from below. Considerable uncertainty still exists over where the resistance to lithospheric deformation comes from, and is likely to be the subject of much future research.

A fascinating possibility discussed by Gourmelen and Amelung (*1*) is the evaluation of past earthquake magnitude based on the characteristics of the postseismic response. This prospect may be more tenu-

Published by AAAS

ous because of the analytical challenge involved in resolving the ambiguity between the offset from the earthquake and the viscoelastic structure. However, this approach adds to the small number of methods available for directly linking seismic and geodetic observations with the goal of understanding the entire earthquake cycle. This work represents a step toward understanding the longest periods of the postseismic response as an integral part of the earthquake process. Given the importance and difficulties of evaluating total earthquake magnitude in events like the 2004/2005 Sumatra great earthquakes, and because much of the energy release and stress transfer from such earthquakes can occur months to decades after the event, any new constraints are welcome. In this way we put the ghosts of earthquakes to good use.

References and Notes

1. N. Gourmelen, F. Amelung, *Science* **310**, 1473 (2005).
2. A. Nur, G. Mavko, *Science* **183**, 204 (1974).
3. L. M. Cathles, in *The Viscosity of the Earth's Mantle* (Princeton Univ. Press, Princeton, NJ, 1975), p. 390.
4. S. M. Nakiboglu, K. Lambeck, *J. Geophys. Res.* **88**, 10439 (1983).
5. B. G. Bills, G. M. May, *J. Geophys. Res.* **92**, 11 (1987).
6. W. Thatcher *et al.*, *Science* **283**, 1714 (1999).
7. Assuming lower crust viscosity $\eta_{LC} = 3.2 \times 10^{20}$ Pa-s and upper mantle viscosity $\eta_{UM} = 10^{19}$ Pa-s, very similar to the best values found by (*1*). Seismic sources are 1915 Pleasant Valley [moment magnitude (M_w = 7.4)], 1954 Dixie Valley (M_w = 6.9), 1954 Fairview Peak (M_w = 7.0) and 1932 Cedar Mountain (M_w = 7.1), and the 1954 Stillwater sequence (combined M_w = 7.0).
8. F. F. Pollitz, *J. Geophys. Res.* **102**, 17921 (1997).
9. J. W. Bell, S. J. Caskey, A. R. Ramelli, L. Guerrieri, *Bull. Seismol. Soc. Am.* **94**, 1229 (2004).
10. A. M. Friedrich, B. P. Wernicke, N. A. Niemi, R. A. Bennett, G. A. Davis, *J. Geophys. Res.* **108**, 2199 (2003).
11. R. A. Bennett, A. M. Friedrich, K. P. Furlong, *Geology* **32**, 961 (2004).
12. J. Deng, M. Gurnis, H. Kanamoori, E. Hauksson, *Science* **282**, 1689 (1998).
13. S. H. Kirby, A. K. Kronenberg, *Rev. Geophys.* **25**, 1219 (1987).
14. L. Block, L. H. Royden, *Tectonics* **9**, 557 (1990).

10.1126/science.1121349

IMMUNOLOGY

Tipping the Scales Toward More Effective Antibodies

Jenny M. Woof

Antibodies are lifesavers par excellence. Not only do these vital proteins of the immune system armory protect millions of people across the globe after being elicited in vaccination programs, but also they serve increasingly as potent therapeutics in the clinic. Monoclonal antibodies, homogeneous antibody preparations specific for single antigens that have long been heralded as magic bullets, are finally fulfilling their promise. Indeed, monoclonal antibodies directed against targets such as cancer cells represent a major focus of the biopharmaceutical industry. But antibodies come in many different classes and subclasses, so how do we decide which category of antibody is most suitable for a particular clinical application? Mouse models of diseases can provide important insights, and a report by Nimmerjahn and Ravetch on page 1510 of this issue (*1*) raises the possibility of predicting the in vivo efficacy of individual immunoglobulin G (IgG) subclasses in treating particular cancers and infections.

IgG, the major immunoglobulin class in serum, exists as four structurally distinct subclasses in humans and mice. All IgG subclasses recognize antigens on foreign cells but have markedly different abilities to trigger immune mechanisms to eliminate these foreign targets. The latter processes rely on interaction of the Fc region of the antibody with effector molecules such as complement in the serum or Fc receptors (FcγRs) expressed on a variety of immune cells. FcγRs also come in different classes (*2*). In humans, there are three types: FcγRI, FcγRII, and FcγRIII. FcγRII is further subdivided into FcγRIIA, FcγRIIB, and FcγRIIC. Although the correspondence is not absolute, mice also have FcγRI, FcγRII, and FcγRIII, along with a recently discovered additional class, FcγRIV, which is absent in humans (*3*). Mice have only the FcγRIIB form of FcγRII.

In terms of function, FcγRs fall into two camps—those that activate a cellular response, and those that block it. Activatory receptors usually associate with a transmembrane signaling component that carries an immunoreceptor tyrosine-based activation motif (ITAM), or in some cases the activatory receptor possesses its own ITAM. In contrast, the single inhibitory receptor FcγRIIB carries a cytoplasmic immunoreceptor tyrosine-based inhibitory motif (ITIM). When one or more FcγRs on an FcγR-positive cell simultaneously bind IgG presented in an aggregated form (e.g., on the surface of a foreign cell), cellular responses are triggered. Engagement of activatory receptors initiates intracellular kinase cascades, culminating in responses such as phagocytosis and release of inflammatory mediators. On the other hand, engagement of both activatory and inhibitory receptors by antigen results in recruitment of intracellular phosphatases that effectively terminate any activation. Because activatory and inhibitory receptors are frequently coexpressed on immune cells such as macrophages and monocytes, the final nature of the cellular response reflects a finely tuned balance between activatory and inhibitory signaling.

How can we better understand the rules

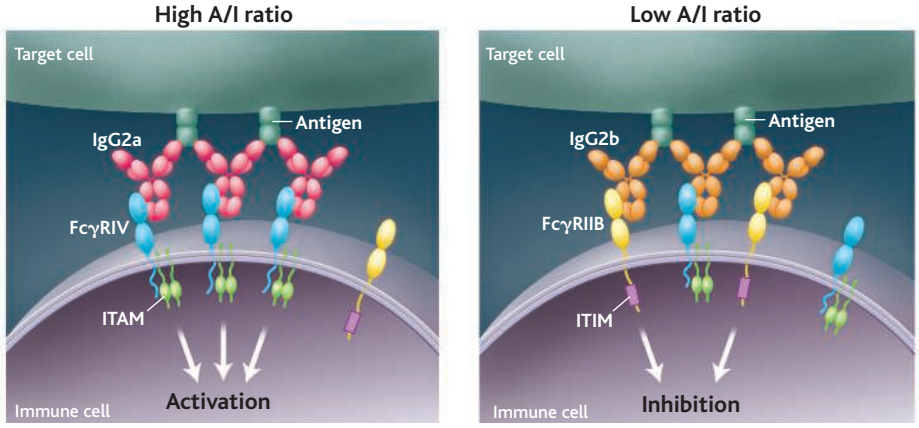

Activation versus inhibition. With a high activatory to inhibitory (A/I) ratio, IgG2a (red) antibody binds antigen (dark green) on a target cell surface and preferentially binds to activatory receptor FcγRIV (blue) rather than to inhibitory receptor FcγRIIB (yellow), and immune cell activation results. In contrast, an IgG2b antibody (orange), with a lower A/I ratio, will bind both FcγRIV and FcγRIIB and activation is dampened.

CREDIT: K. SUTLIFF/*SCIENCE*

The author is in the Division of Pathology and Neuroscience, University of Dundee Medical School, Ninewells Hospital, Dundee DD1 9SY, UK. E-mail: j.m.woof@dundee.ac.uk